Chapter 8

Discussion and Outlook

In the following concluding discussion, I want to highlight the areas where the new spectrometer opens up new possibilities for interesting measurements, and point out which parts of the equipment should be improved to fully exploit its potential.

In the motivation (chapter 3), the enhancement of g–factor resolution was put forth as one of the major reasons to perform EPR at high fields and high frequencies. It was also mentioned, that in some cases field–dependent line–broadening can drastically reduce this effect. A very straightforward way to see, whether this is the case for the measurements in this work, is to compare two spectra obtained both at 360 GHz and at W–band. In contrast to the illustrative example given in figure 7.5, in figure 8.1 both spectra are plotted against a g–factor axis. This lets one directly compare the width of the spectral features corresponding to the principal values of the **g**–tensor. From this figure it immediately becomes apparent that the 360 GHz spectrum indeed exhibits a smaller linewidth on a g–factor axis. Since the magnitude of the hyperfine splittings is field independent, in the 360 GHz spectrum on a g–axis they appear compressed.

With the spectral resolution of the g–tensor at 360 GHz so obviously being higher than at W–band, the direct conclusion can be drawn that the current

measurement uncertainty quoted for the measured g–values of nitroxides of ±0.00005 for the g_{zz}–component and ±0.0001 for the g_{xx}–component can be greatly improved by a better calibration of the magnetic field. To this end, the first experiments with the new probehead (figure 5.6) show great promise since due to the reduced microphonics effect, the stability of the resonator was improved, allowing for smaller field sweep rates and therefore better resolution of the Mn^{2+} field standard lines. This will reduce the error of the nonlinear interpolation of the Mn^{2+} resonance positions described in section 7.1. It is anticipated that with this improvement, the error in the deter-
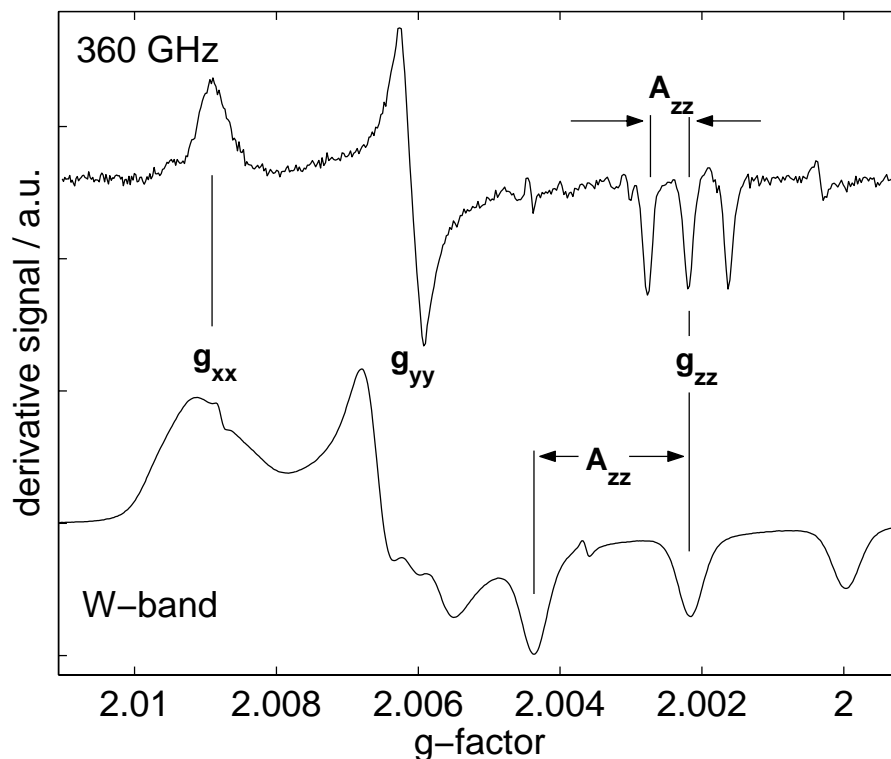

Figure 8.1: 4–hydroxy–TEMPO in water/glycerol ($T = 200$ K) at 360 GHz, compared to a spectrum of an identical sample at W–band (95 GHz). The spectra are identical to those in figure 7.7 (360 GHz spectrum) and figure 7.5 (W–band spectrum). The weak narrow lines superimposed in both spectra are the hyperfine lines of the Mn^{2+} field standard.

mination of absolute g–values should become $\pm$ 0.00002 or smaller for lines situated within the Mn^{2+} hyperfine spectrum. The main error contribution would then be due to the precision of the field standard itself.

To be able to determine to higher precision the g–values of resonance positions shifted to higher or lower fields than the Mn^{2+} spectrum, different measures have to be taken. One way would be to find a different standard sample that exhibits lines with a g–value of at least 2.008 or higher. The other way would be to measure the nonlinearity of the field sweep directly with an NMR gaussmeter. The field axis can then be calibrated absolutely at one point to a Mn^{2+} resonance line and the relative field variation around this line can be obtained from the gaussmeter measurement. Since the probe-head of our NMR gaussmeter is too bulky to be inserted together with the EPR probehead, field profiles for several reference field ranges and sweep frequencies will have to be gathered separately. Under the assumption that the nonlinearity of the field sweep depends reproducibly on the sweep range and sweep rate this would yield a reliable calibration curve. Instead, the magnetic field could be monitored together with the EPR measurement and the linear offset to the actual field could be taken with reference to a standard. Which one of these approaches will work best remains to be evaluated.

The improved stability and reduced microphonics effects due to the new setup of the resonator probehead mentioned above also suggest that the absolute sensitivity of the spectrometer has improved, since the strong vibrations due to the field modulation coils were considered the noise determining factor of the previous setup. This should be verified in a future measurement.

It was shown in a first measurement of a spin–labeled protein (bacteriorhodopsin mutant V167C, figure 7.10), that the spectrometer sensitivity is high enough to allow for high–resolution g–factor measurements of bioorganic samples in frozen solution. This specific example did not yet require the move to a detection frequency of 360 GHz, since its **g**–tensor already
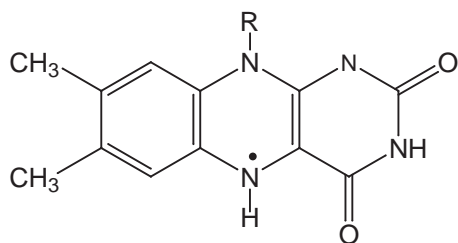
Figure 8.2: Structure of the neutral flavin radical FADH$^\bullet$

meets the high–field condition (equation 3.3) in W–band.

A sample that has been measured both in X–band and W–band by continuous wave and pulsed EPR and ENDOR techniques is the neutral flavin radical FADH$^\bullet$ in the DNA repair enzyme DNA photolyase of Escherichia coli shown in figure 8.2 (Kay et al. 1999). In this case, the **g**–tensor resolution even at W–band frequency is not enough to fully resolve the primary components (figure 8.3). From a preliminary fit the values were determined
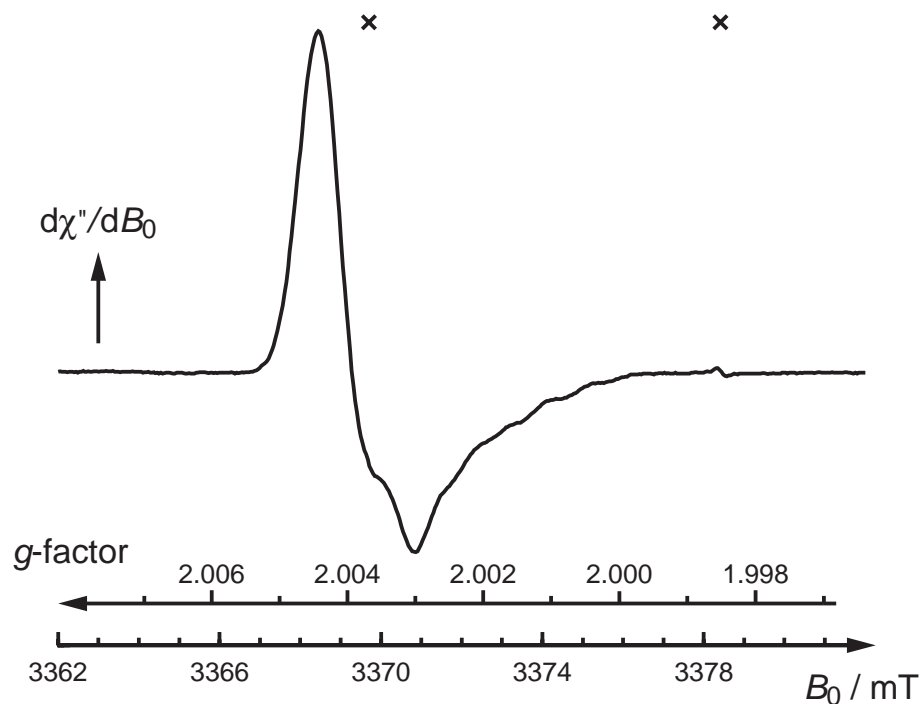

Figure 8.3: W–band EPR spectrum of the neutral flavin radical FADH$^\bullet$. The crosses mark the hyperfine lines of the Mn^{2+} field calibration standard. Figure courtesy of S. Weber (Kay et al. 1999).

to $g_\perp = 2.0043$ and $g_\parallel = 2.0022$. A possible small anisotropy of the $g_\perp$–component could not be resolved with high enough precision. A measurement at 360 GHz should be able to fully resolve the **g**–tensor and probably even resolve the low field components contained in $g_\perp$. A determination of the **g**–tensor components to a precision one order of magnitude higher reduces the number of free parameters in simulations of the X– and W–band spectra. This example shows that often only a multi–frequency approach will yield a complete parameter set of a sample.

As far as the technical side of the measurements at 360 GHz is concerned, an extension of the spectrometer to pulsed operation is in progress. The pulsed source will be a Smith–Purcell free electron laser, also called "orotron". An extensive review of its principle of operation can be found in (Wortman & Leavitt 1983). The development of this device for an operating frequency of 360 GHz is done in collaboration with Y. Grishin and B. Dumesh.

A central requirement for pulsed EPR spectroscopy is a high microwave field B_1 at the sample position to obtain short pulses. With its lower conversion factor and lower filling factor in comparison to a single mode cylindrical resonator, the Fabry–Perot resonator of the current spectrometer setup is not an ideal solution. Considering the recent positive experiences with building a single mode cavity for 300 GHz in the high–field EPR workgroup of J. Schmidt in Leiden (Disselhorst & Schmidt 1999), Netherlands, the development of a similar single mode cylindrical resonator for 360 GHz is planned.

Since the current transmission line setup of our spectrometer is designed for induction mode operation (subsection 5.2.2), it will have to be modified to operate with a single mode cavity. The reason for this is that the separation of excitation microwave and EPR signal in the induction mode setup utilizes the two orthogonal polarization states of the microwave field that are not supported by a single mode resonator. It is possible, however, by use of
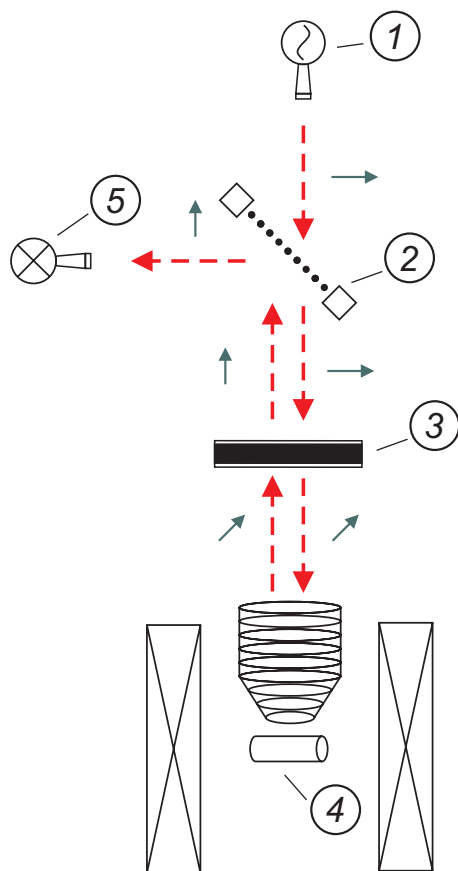
Figure 8.4: Transmission line setup with a quasi optical circulator: The general setup will be identical to figure 5.4, with changes shown here: source (1), wire grid polarizer (2), 45° Faraday Rotator (3), cylindrical single mode resonator (4), detector (5). The dashed arrows indicate the beam path, the small solid arrows indicate the polarization directions. On the way to the cavity (4), the beam passes the Faraday rotator (3) twice, with a resultant rotation of polarization of 90°. The grid polarizer (2) that was initially passed, now acts as a mirror and reflects all microwave power onto the detector.

a so–called Faraday Rotator, to construct a quasi optical analogon to the circulator device used in conventional EPR (Smith et al. 1998). Its priciple of operation is briefly sketched in figure 8.4. The relative ease with which such a fundamental change in transmission line setup can be achieved should demonstrate the extreme flexibility of the quasi optical techniques.

These modifications to the spectrometer will allow us to gain first experiences at 360 GHz with pulsed EPR and ENDOR techniques, that have proven extremely fruitful at frequencies up to around 140 GHz and have been successfully demonstrated at frequencies up to 600 GHz (Moll et al. 1999)